DOI: https://doi.org/10.31351/vol28iss2pp151-158

Design, Synthesis and Cytotoxicity Study of Primary Amides as Histone Deacetylase Inhibitors

Duraid Al-Amily*,1 and Mohammed H. Mohammed*

*Department of Pharmaceutical Chemistry, College of Pharmacy, University of Baghdad, Baghdad, Iraq.

Abstract

Primary amide derivatives as histone deacetylase inhibitors (HDACIs) are very rare. This paper describes the synthesis of the primary amide derivatives adipic monoanilide amide and pimelic monoanilide amide (compounds **6** and **7**) that have the requirements to be histone deacetylase inhibitors of the zinc-binding type. Both of them exhibited good cytotoxicity against the tested cancer cell lines with much lower cytotoxicity against normal cell line.

Keywords: Primary amides, HDACIs, Adipic monoanilide amide, Pimelic monoanilide amide

تصميم، تخليق، و دراسة السمية الخلوية للأمايدات الاولية كمثبطات لأنزيم الهيستون دي اسيتيليز

دريد حامد العاملي *،١ و محمد حسن محمد*

فرع الكيمياء الصيدلانية، كلية الصيدلة، جامعة بغداد، بغداد، العراق.

الخلاصة

تعتبر مشتقات الامايد الاولية المثبطة لأنزيمات الهيستون دي اسيتيليز نادرة. و عليه، فقد تم تخليق مشتقي أمايد اولي (المركبين ٦ و ٧) و المتضمنين للمتطلبات اللازمة لجعلهما من مثباطات هذه الانزيمات التي ترتبط بالزنك. و قد اظهر هذين المركبين سمية جيدة ضد الخلايا السرطانية و ضعيفة ضد الخلايا الطبيعية.

الكلمات المفتاحية: امايدات اولية، مثبطات الهيستون دي اسيتيليز، امايد الادبك احادي الانالايد، امايد البايميليك احادي الانالايد.

Introduction

Histone deacetylases (HDACs) are a group of enzymes responsible for the deacetylation of the ε-amino groups of lysine residues at the N-termini of histones [(1)], the core proteins that serve to compact DNA into nucleosomes which comprise chromatins [(2)]. The deacetylation process encourages the compaction of nucleosomes and repression of gene transcription [(3)]. Many reports demonstrate that HDACs are overexpressed in several types of cancer [(1,4)]. Therefore , they are considered as valuable targets for cancer treatment [(5)].

Eighteen isoforms of HDACs have been identified in mammalian tissues. They fall into four major classes (I-IV). Class I includes HDAC1, 2, 3, and 8 while class II includes isoforms 4-7, 9 and 10. Isoform 11 represents class IV. These three classes have a zinc-dependent catalytic site. The rest seven isoforms depend on the cofactor nicotine adenine dinucleotide rather than zinc for their catalytic activity and comprise class III [(6)].

The zinc-dependent classes are highly investigated and subjected to inhibition studies as an approach for cancer treatment [(7)]. A classical and popular example is HDAC2 since its crystallographic structure is well resolved [(8)]. Previous studies on the binding site revealed that it is shaped as an internal tubular (tunnel) cavity having a length of 11 Å. At the bottom of this cavity lies a zinc ion followed by a 14 Å foot-like pocket [(9)] (Figure 1). Lysine residues of histone fit into the tunnel so that they could be deacetylated [(3)].

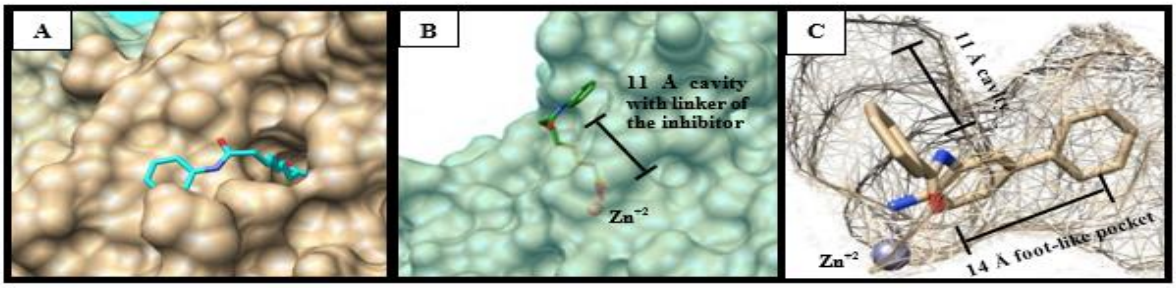

Figure 1 .The binding site of HDAC2. (A): The opening of the tunnel cavity is shown in which the linker of the inhibitor (cyan) is lying. (B): A side view of the binding site with 30% transparency of the surface to make the whole length of the tunnel (11 Å) visible together with the linker of the inhibitor (forest green). Zinc ion is visible at the deepest end of the tunnel. (C): Mesh surface of the binding site showing the inhibitor inside the 14 Å foot-like pocket.

[1]Corresponding author E-mail : colrelated@copharm.uobaghdad.edu.iq
Received: 31/ 5 /2019
Accepted: 21/8 / 2019

Accordingly, the design of inhibitors for zinc-dependent HDACs should have a zinc binding group (ZBG) to bind to the zinc ion, a linker of 4-6 carbon atoms length to fit into the cavity, and a hydrophobic cap to recognize and interact with the outer surface [(1)]. These are best illustrated by the classical inhibitor suberoylanilide hydroxamic acid **1** (SAHA, vorinostat) [(10)].Other known synthetic inhibitors with ZBG other than hydroxamic acid derivatives include entinostat **2** (MS-275), a benzamide, and valproic acid **3** [(5)] (Figure 2)**.** Among other rare synthetic ZBG are the secondary amide derivative **4** [(11,12)] and the only primary amide **5** mentioned in the literature that showed an IC_{50} against HDAC1 in a nanomolar concentration [(13)] .

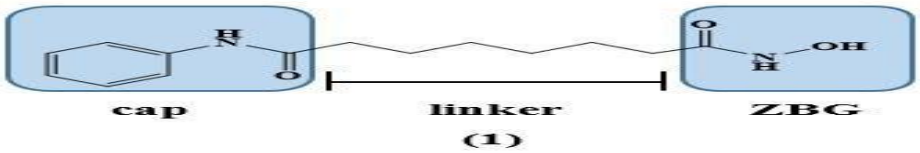

(1)

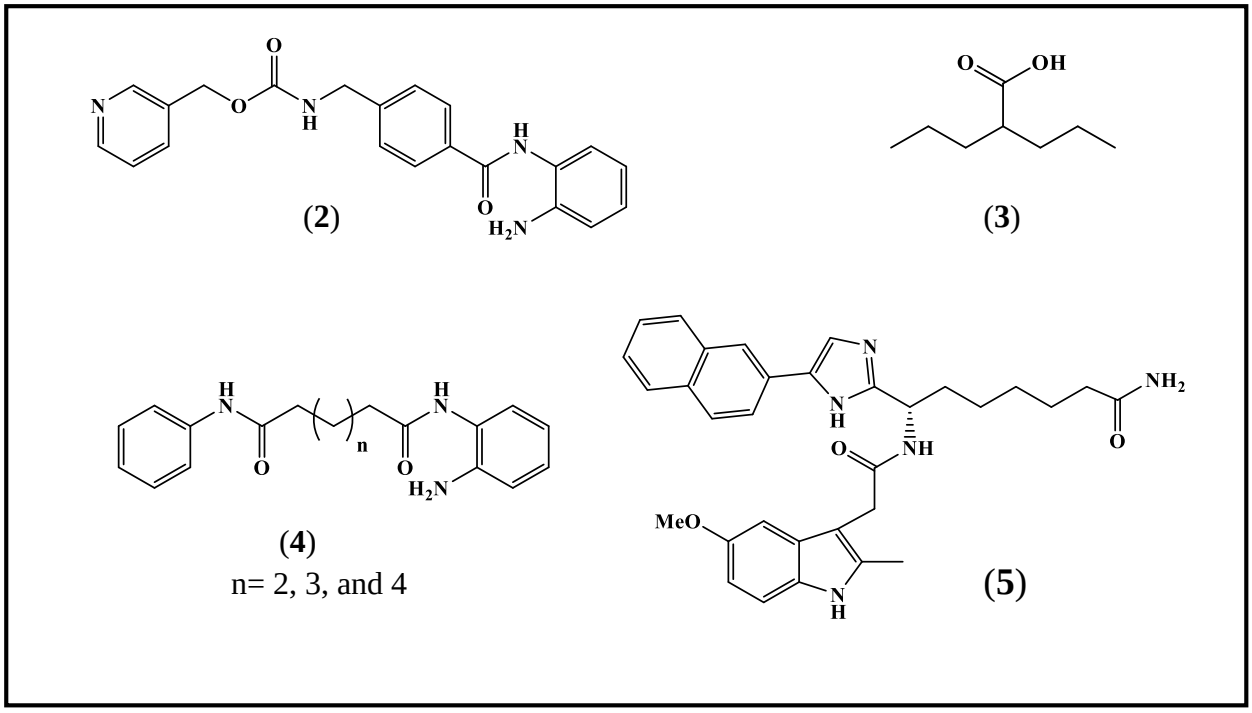

Figure2. Examples of HDAIs with different ZBGs

Here, we wish to describe the synthesis of the small and simple primary amide molecules **6** and **7** that fulfill the three requirements for zinc-dependent HDAC inhibitors.

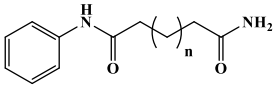

(**6**) n= 2
(**7**) n= 3

Besides, we'll mention the results of the *in vitro* cytotoxicity assay for these compounds against HRT-18 cell line (human colon adenocarcinoma) and HC-04 cell line (mouse hepatic carcinoma).

Materials and Methods

Reagents and solvents were used for chemical synthesis as obtained from the supplier (Sigma-Aldrich, Fluka, Romil, GCC Diagnostics, ReagentWorld, and Thomas-Baker). Melting points were measured using the Stuart SMP3 melting point apparatus (UK) and are uncorrected. Thin-layer chromatography was achieved using 0.2 mm pre-coated TLC-sheets Alugram® Xtra SIL G/UV254 (Macherey-Nagel, Germany) and the visualization was under a 254 nm UV lamp. FT-IR spectroscopy was done using Shimadzu IRAffinity-1 Spectrometer (Shimadzu, Japan) and Specac® Quest ATR- diamond type (UK) at the University of Baghdad-College of Pharmacy. ^{1}H-NMR and ^{13}C-NMR analysis was performed at 400 MHz and 100 MHz respectively (d_6 - DMSO as the solvent) using

The Bruker Avance III, 400 MHz spectrometer (USA) at Sophisticated Test and Instrumentation Centre (Cochin University of Science and Technology-India), with the chemical shifts (δ) expressed in parts per million.

Figures illustrating the binding site of HDACs and the binding of the ligand were captured using UCSF Chimera [14] and the PDB (www.rcsb.org) [15] files with IDs 4LXZ [8] and 3MAX [16].

Cytotoxicity assay was performed at the iRAQ Biotech laboratories using trypsin/EDTA, RPMI 1640, fetal bovine serum (Capricorn, Germany); 3- (4 , 5 – dimethyl – 2 - thiazolyl) -2,5-diphenyl-2H-tetrazolium bromide (MTT stain- Bio-World, USA); dimethyl sulfoxide (DMSO-Santacruz Biotechnology, USA); CO_2 incubator and laminar flow hood (Cypress Diagnostics, Belgium); microtiter reader (Gennex lab., India); cell culture plates (Santa Cruz Biotechnology, USA).

***Chemical synthesis* (scheme 1)**

***General synthesis of adipic and pimelic anhydrides* (6b and 7b)**

Adipic acid (**6a**) or pimelic acid (**7a**) (27.4 mmol of each) was suspended in acetic anhydride (3 mL/g) and refluxed for 1 hour. The solvent was then evaporated under reduced pressure to obtain a semisolid mixture of **6b** and **6c**, or **7b** and **7c,** which was used as such in the next step. FT-IR (ATR; υ, cm^{-1}): 1801, 1739 for **6b** and 1813, 1743 for **7b** (sym. and asym. C=O respectively).

General synthesis of monosodium adipic monoanilide and monosodium pimelic monoanilide (6d and 7d)

The obtained mixture of compounds **6b** and **6c**, or **7b** and **7c** was dissolved in 10 mL of dry DMF in a round bottom flask that was equipped with calcium chloride tube and cooled to 0 ˚C. Then 3 mL of aniline (32.88 mmol) were added gradually with continuous stirring and cooling. The mixture was then kept stirred at room temperature for 24 hours. The mixture was then acidified with 5 N hydrochloric acid, diluted to about 300 mL with cold water, and the precipitate formed was then filtered. The precipitate was washed with water (3×50 mL). Then it was suspended in no more than 50 mL of ice-cooled water and the pH of this mixture was raised to 7 by a drop wise addition of 0.5 N sodium hydroxide solution at 0 ˚C. The mixture was stirred for 30 minutes at 0 ˚C while maintaining this pH by addition of 0.5 N sodium hydroxide solution as needed. Then the mixture was filtered and the filtrate was evaporated to dryness.

Compound **6d**: off-white powder, yield 35% relative to **6a**, m. p. 259.5-263.8 ˚C. FT-IR (ATR; υ, cm^{-1}): 3332 (aromatic NH), 3062 (aromatic C-H), 2939 (asym CH_2), 2866 (sym. CH_2), 1666 (amide C=O), 1600 (aromatic C=C)1562 (asym carboxylate C=O), 1539 and 1500 (aromatic C=C), 1431 (sym. carboxylate C=O).

Compound **7d**: off-white powder, yield 25.5% relative to **7a**, m. p. 214-217 ˚C. FT-IR (ATR; υ, cm^{-1}): 3290 (aromatic NH), 3078 (aromatic C-H), 2920 (asym. CH_2), 2858 (sym. CH_2), 1654 (amide C=O), 1597 (aromatic C=C), 1558 (asym. carboxylate C=O), 1543 and 1496 (aromatic C=C), 1435 (sym. carboxylate C=O).

***General synthesis of adipic monoanilide acid chloride and pimelic monoanilide* acid chloride (6e and 7e)**

Compound **6d** or **7d** (4 mmol) was suspended in 15 mL dry dichloromethane in a round bottom flask that was equipped with calcium chloride tube and cooled in an ice bath. Pyridine (4 mmol, 0.32 mL) was added followed by a drop wise addition of 0.34 mL of thionyl chloride (4.8 mmol) with continuous stirring and cooling for 10 minutes. The mixture was then allowed to warm to room temperature with continuous stirring for 30 minutes. Then the precipitate formed was collected using Büchner funnel. The precipitate was washed with dry dichloromethane (3×10 mL) during filtration. The white solid mass obtained (in both cases of **6e** and **7e**) was used as such in the next step.

Compound **6e** FT-IR (ATR; υ, cm^{-1}): 3313 (aromatic NH), 3066 (aromatic C-H), 2935 (asym. CH_2), 2870 (sym. CH_2), 1797 (acid chloride C=O), 1662 (amide C=O), 1600, 1535 and 1500 (aromatic C=C).

Compound **7e** FT-IR (ATR; υ, cm^{-1}): 3313 (aromatic NH), 3043 (aromatic C-H), 2939 (asym. CH_2), 2870 (sym. CH_2), 1797 (acid chloride C=O), 1662 (amide C=O), 1597, 1527 and 1500 (aromatic C=C).

***General synthesis of adipic monoanilide amide and pimelic monoanilide* amide (6 and 7)**

The precipitate obtained from the previous step (**6e** or **7e)** was suspended in 10 mL of anhydrous cold acetone and added gradually to 10 mL of concentrated aqueous ammonium hydroxide solution that was cooled in an ice bath. The mixture was stirred for 30 minutes while maintained in the ice bath, then extracted three times with 5 mL-portions dichloromethane. The organic phase was evaporated to dryness under reduced pressure.

Compound **6**: white powder, yield 65% (relative to **6d**), m. p. 178.2- 179.3 °C, R_f 0.34 (dichloromethane: 1-propanol; 8:2). FT-IR (ATR; υ, cm^{-1}): 3390 (asym. aliphatic NH) 3305 (aromatic NH), 3194 (sym. aliphatic NH), 3043 (aromatic C-H), 2951 (asym. CH_2), 2873 (sym. CH_2), 1643 (br, aliphatic and aromatic amide C=O), 1597, 1523 and 1500 (aromatic C=C).

^{1}H-NMR (δ, ppm): 1.54 (m, -CH_2-CH_2-, 4H), 2.07 (t, aliphatic -CH_2-C(O)-, 2H), 2.29 (t, aromatic -CH_2-C(O)-, 2H), 6.71 (br, -NH_2, 1H), 7.02 (t, *p*-CH, 1H), 7.28 (t, *m*-CH, 2H; and -NH_2, 1H), 7.58 (d, *o*-CH, 2H), 9.86 (s, -NH-1H).

^{13}C-NMR (δ): 24.78, 24.87, 34.90, 36.23, 119.03, 122.94, 128.60, 139.24, 171.15, 174.26.

Compound **7**: gray crystals, yield 55% (relative to **7d**), m. p. 127- 129 °C, R_f 0.42 (dichloromethane: 1-propanol; 8:2). FT-IR (ATR; υ, cm^{-1}): 3367 (asym. aliphatic NH) 3313 (aromatic NH), 3174 (sym. aliphatic NH), 3043 (aromatic C-H), 2939 (asym. CH_2), 2854 (sym. CH_2), 1658 (br, aliphatic and aromatic amide C=O), 1597, 1523 and 1496 (aromatic C=C).

^{1}H-NMR (δ): 1.28 (t, -CH_2- 2H), 1.54 (m, -CH_2-CH_2- , 4H), 2.04 (t, aliphatic -CH_2-C(O)-, 2H), 2.29 (t, aromatic -CH_2-C(O)-, 2H), 6.68 (br, -NH_2, 1H), 7.01 (t, *p*-CH, 1H), 7.28 (t, *m*-CH, 2H; and -NH_2, 1H), 7.58 (d, *o*-CH, 2H), 9.85 (s, -NH-1H).

^{13}C-NMR (δ): 24.85, 24.89, 28.31, 34.94, 36.27, 119.02, 122.92, 128.60, 139.25, 171.24, 174.37.

Maintenance of cell cultures

HRT-18, HC-04, and HBL-100 (epithelial cells obtained from healthy human breast milk) cell lines were maintained in RPMI-1640 medium with which 10% fetal bovine was supplemented, 100 units/mL penicillin, and 100 µg/mL streptomycin. The cells were subcultured using Trypsin-EDTA, reseeded, once getting 80% confluence, two times a week, and incubated at 37 °C [17].

Cytotoxicity assay

MTT cell viability assay was done using 96-well plates. The chosen cell lines were seeded at 1 × 10^4 cells/well. After either 24 hours or a confluent monolayer had been obtained, the cells were treated with compounds **6** or **7** at different concentration (6.25, 12.5, 25, 50, 100 µM). After a 72 hours- treatment period, the cell viability was measured by removing the medium, adding 28 µL of 2 mg/mL solution of MTT stain and incubating the cells for 2.5 hours at 37 °C. Then the MTT solution was removed and the remaining crystals in the wells were dissolved in 130 µL of dimethyl sulfoxide followed by 37 °C incubation for 15 minutes with shaking [18)]. The absorbency was determined on a microplate reader at 492 nm; the assay was performed in triplicate.

The inhibition rate of cell growth (the percentage of cytotoxicity) was calculated according to the following equation:

$$Cytotoxicity\ (\%) = \frac{A - B}{A} \times 100$$

where A is the optical density of the control and B is the optical density of the sample.

The morphology of cells was visualized by the aid of inverted microscope. 200 µL of cell suspensions were seeded in 96-well micro-titration plates at density 1x10^4 cells/ mL and incubated for 48 hours at 37 °C. After removing the medium, compound **6** or **7** was added at the (IC_{50}). Then, after the exposure time, 50 µL of crystal violet were used to stain the plates which were incubated at 37 °C for 15 min; gentle washing of the stain was done with water until no more dye remained. A 40x magnification of inverted microscope was selected to examine the cells; they were photographed with a digital camera.

Statistical analysis

Unpaired t-test (using GraphPad Prism 6) was applied for the statistical analysis of the collected data. The values were presented as the mean ± SEM of triplicate measurements.

Results and discussion

Chemical synthesis

Synthesis of the target compounds (**6** and **7**) was started from adipic acid (**6a**) and pimelic acid (**7a**) respectively (Scheme 1). Heating these dicarboxylic acids in acetic anhydride for 1 hour would result in monomeric cyclic anhydrides (**6b** and **7b**). However, these anhydrides are extremely unstable and some of the synthesized amount is converted into polymeric anhydrides (**6c** and **7c**) rapidly during evaporation of the solvent [11,19]. The anhydride mixture (**6b** and **6c**, or **7b** and **7c**) was used as such in the next step which is a modified procedure from previously published works [20,21]. In this step, a slight excess of aniline (1.2 eq. relative to **6a** and **7a**) was added gradually to an ice-cooled solution of the anhydride mixture (in dry DMF) and, then, stirred at room temperature for 24 hours. The sodium salts (**6d** and **7d**) were obtained by treatment of the precipitate, resulted after cold acidification of the reaction mixture and filtration, with gradually increasing amounts of ice-cooled NaOH solution (0.5 N) so that the pH was not raised above 7. After filtration and evaporation to dryness, the off-white precipitate (**6d** and **7d**) showed the characteristic FT-IR amide peaks (respectively) at 3332 cm^{-1} and 3290 cm^{-1} (aromatic NH) and at 1666 cm^{-1} and 1654 cm^{-1} (amide carbonyl). Furthermore, the carboxylate peaks were at 1562 cm^{-1} (asym. C=O) and 1431 cm^{-1} (sym. C=O) for **6d** and at 1558 cm^{-1} (asym. C=O) and 1435 cm^{-1} (sym. C=O) for **7d**. These anilides were prepared as sodium salts in order to keep the amide function stable during the next step which involved the synthesis of the acid chlorides **6e** and **7e** using thionyl chloride in the presence of 1 equivalent of pyridine [22], thus avoiding the liberation of HCl. Both **6e** and **7e** showed a new characteristic FT-IR carbonyl peak (of acid chloride) at 1797 cm^{-1} with the disappearance of all of the carboxylate peaks.

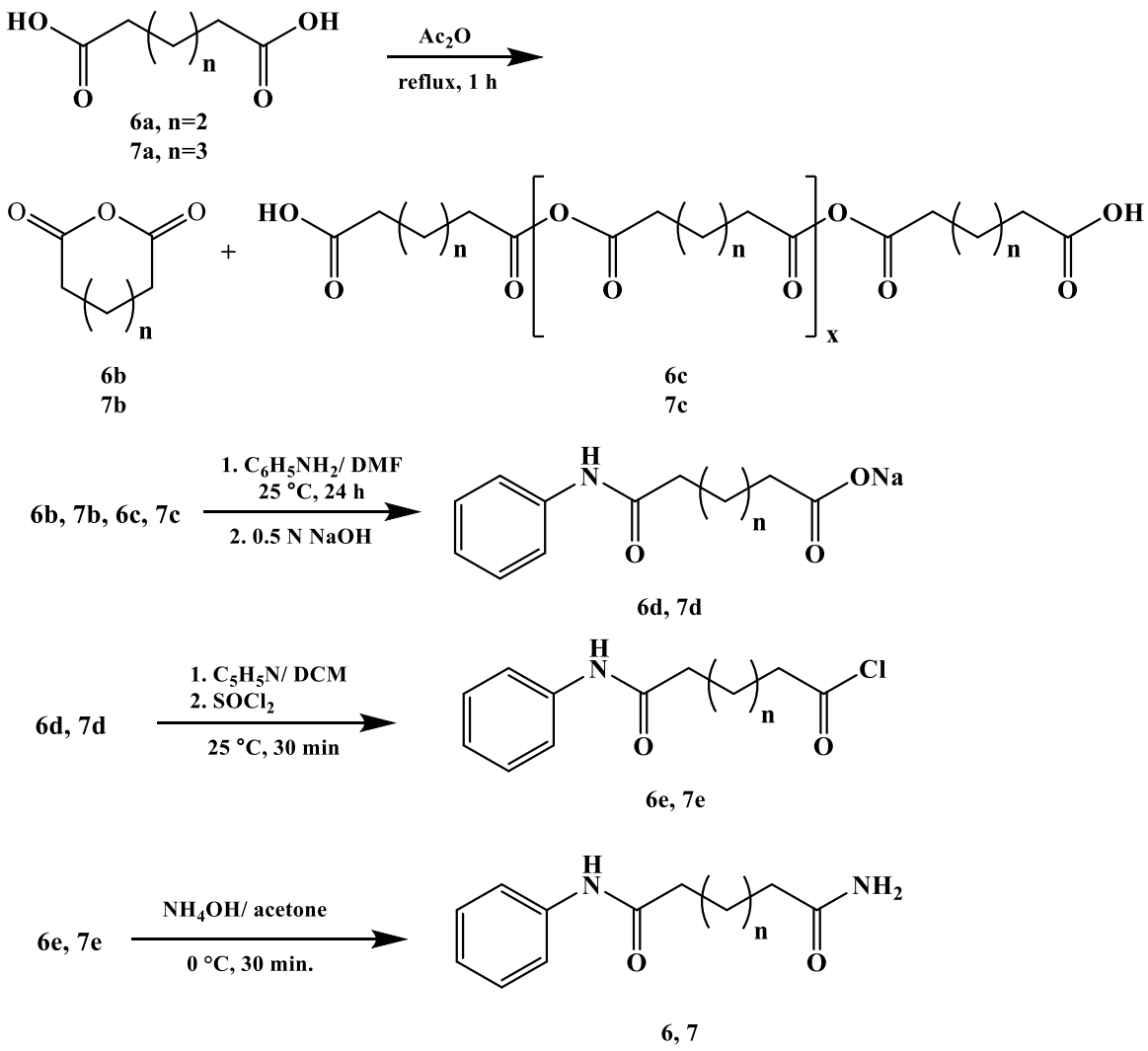

Scheme 1. Synthesis of the target compounds (6 and 7)

The final step of synthesis involved primary amide formation (**6** and **7**) by modifying a simple procedure using ice-cooled concentrated aqueous ammonia solution [23]. The FT-IR spectrum showed the disappearance of the 1797 cm^{-1} peak for both **6** and **7** while the amide carbonyl peaks (1643 cm^{-1} and 1658 cm^{-1}, respectively) became broad because of the overlap of the primary and secondary amide carbonyl groups.

The two protons attached to the nitrogen of the primary amide are chemically not equivalent due to hindered amine rotation [24]. This is illustrated by the difference in their chemical shifts in the ^{1}H-NMR spectrum of **6** and **7** (0.57 ppm and 0.6 ppm respectively).

Cytotoxicity study

Compounds **6** and **7** were tested *in vitro* for antiproliferative activity against HRT-18 cell line (human colon adenocarcinoma), HC-04 cell line (mouse hepatic carcinoma), and HBL-100 cell line (epithelial cells obtained from healthy human breast milk) at micromolar concentrations (6.25, 12.5, 25, 50, 100 µM). Both of them showed inhibitory activity against the cancer cell lines higher than against the normal cell line. Figures 3 and 4 show that there is a continuous and parallel increase in the inhibition of growth of both compounds against both colon adenocarcinoma and hepatic carcinoma with increasing the concentration. On the other hand, they show very low cytotoxicity against normal cells.

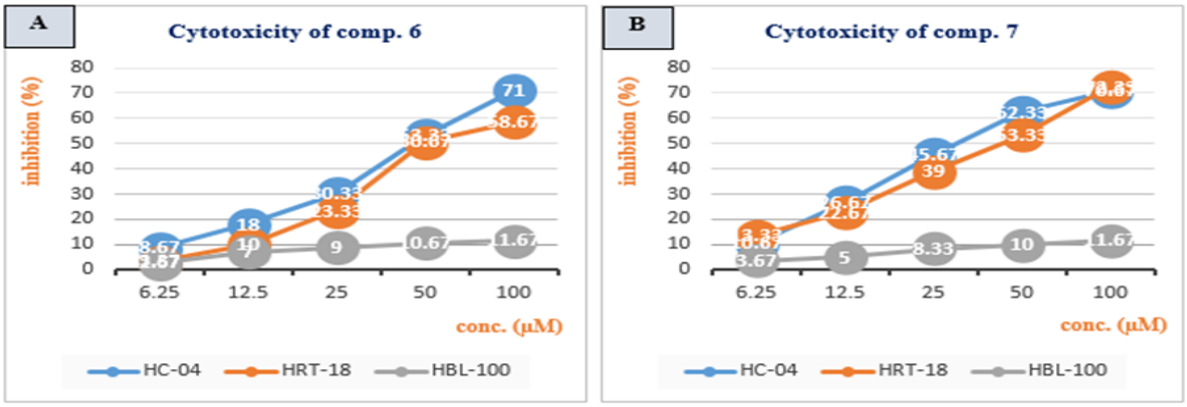

Figure 3. Concentration-growth inhibition curve of the tested compounds against hepatic carcinoma cells (blue), colon adenocarcinoma (orange) and healthy breast cells (gray). (A): the cytotoxicity of compound 6. (B): the cytotoxicity of compound 7

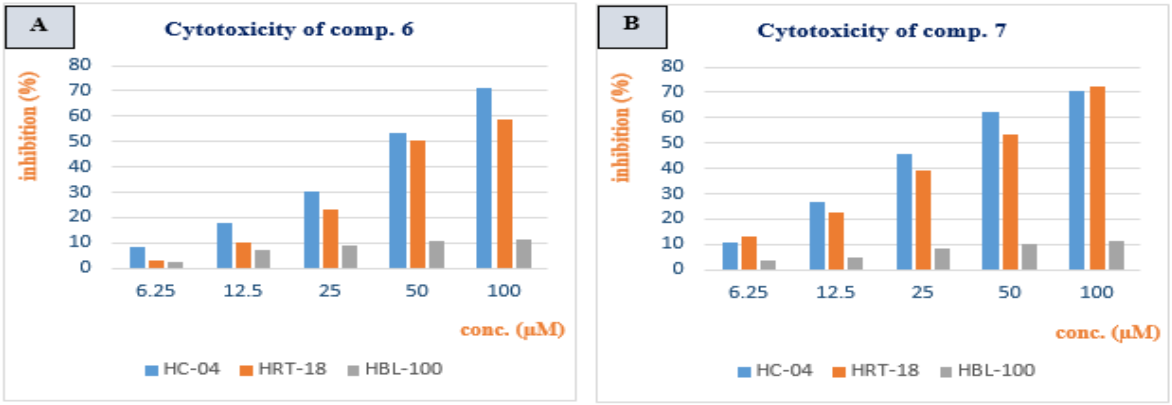

Figure 4. Histogram showing the concentration and growth inhibition of the tested compounds against hepatic carcinoma cells (blue), colon adenocarcinoma (orange) and healthy breast cells (gray). (A): the cytotoxicity of compound 6. (B): the cytotoxicity of compound 7

Compound **7** shows higher cytotoxicity than compound **6** against the tested cancer cells (Figure 5). Its IC_{50} against HC-04 cell line and HRT-18 cell line are 29.43 µM and 33.92 µM respectively while those for compound **6** are 45.83 µM and 47.93 µM. Figure 6 (captured at the IC_{50}) shows the difference in the magnitude of cytotoxicity between the two compounds.

.

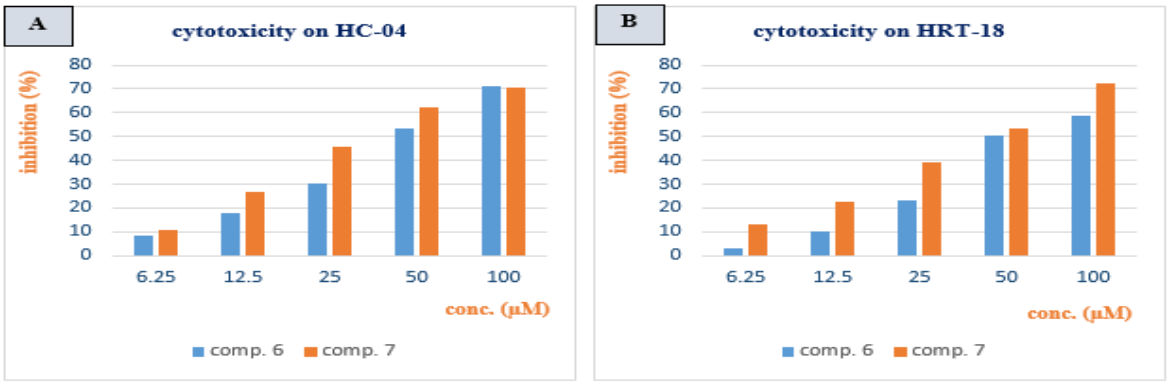

Figure 5. Histogram showing the concentration and growth inhibition of the compounds 6 and 7, (A): against hepatic carcinoma cells and (B): against colon adenocarcinoma

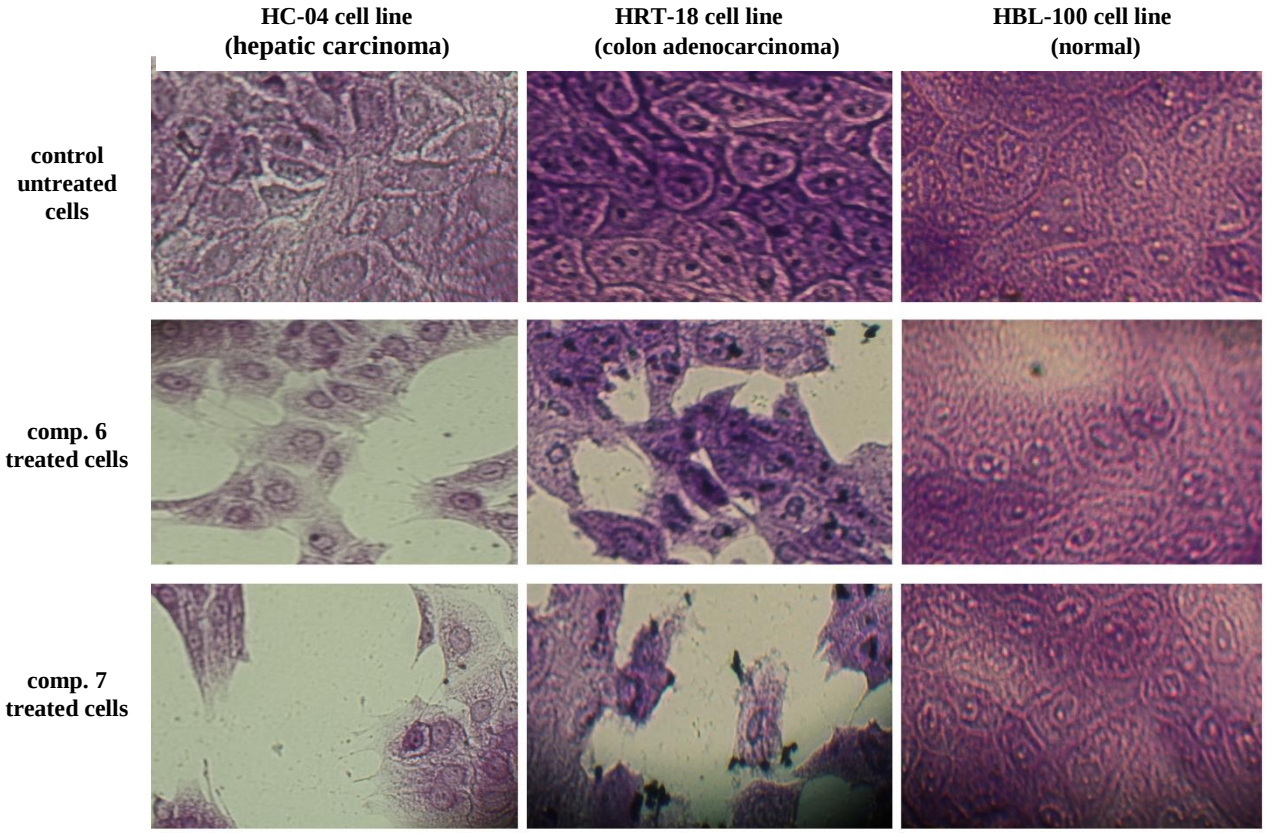

Figure 6. Morphology of the cell lines after treatment with compounds 6 and 7 at the IC_{50} (40x magnified)

The low cytotoxicity of both compounds against normal cells gives hope of being able to target cancer cells to a higher degree than normal cells. No more than 12 % of inhibition of growth was observed at the highest concentration used for both compounds (Figure 7). This might possibly be considered, in agreement with previous reports, that the synthesized compounds might exhibit relative specificity in inhibiting HDACs that are overexpressed in cancer cells.

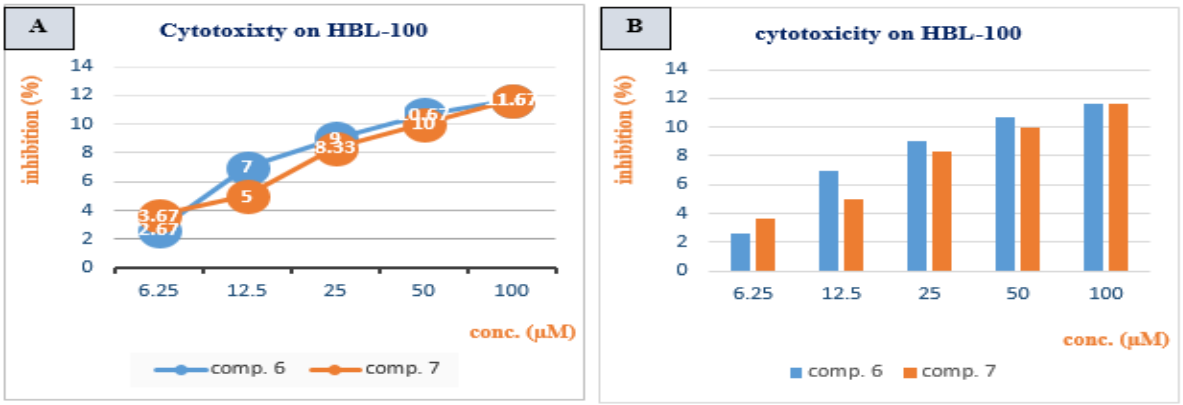

Figure 7. Low cytotoxicity of compounds 6 and 7 on normal breast cells. (A): Concentration-growth inhibition curve. (B): Histogram showing the concentration and growth inhibition

Conclusion

Synthesis of the target primary amides (**6** and **7**) was achieved starting from adipic acid (**6a**) and pimelic acid (**7a**) respectively . They were fully characterized successfully. Both of them showed good cytotoxicity against cancer cell lines (HC-04 and HRT-18) and lower cytotoxicity against normal cell line (HBL-100).

References

1. Delcuve GP, Khan DH, Davie JR. Targeting class I histone deacetylases in cancer therapy. Expert Opin Ther Targets. 2012;17(1):29–41.

2. Burtis CA, Ashwood ER, Bruns DE. Tietz Textbook of Clinical Chemistry and Molecular Diagnostics. Fifth. Missouri: ELSEVIER; 2012. 1212-1214 p.

3. Manal M, Chandrasekar MJN, Gomathi Priya J, Nanjan MJ. Inhibitors of histone deacetylase as antitumor agents: A critical review. Bioorg Chem. 2016;67:18–42.

4. RUIJTER AJM de, GENNIP AH van, CARON HN, KEMP S, KUILENBURG ABP van. Histone deacetylases (HDACs): characterization of the classical HDAC family. Biochem J. 2003;370(3):737–49.

5. Zhang L, Zhang J, Jiang Q, Zhang L, Song W. Zinc binding groups for histone deacetylase inhibitors. J Enzyme Inhib Med Chem. 2018;33(1):714–21.

6. Traoré MDM, Zwick V, SimoÌes-Pires CA, Nurisso A, Issa M, Cuendet M, et al. Hydroxyl Ketone-Based Histone Deacetylase Inhibitors to Gain Insight into Class i HDAC Selectivity versus That of HDAC6. ACS Omega. 2017;2(4):1550–62.

7. Kim H-J, Bae S-C. Histone deacetylase inhibitors: molecular mechanisms of action and clinical trials as anti-cancer drugs. Am J Transl Res. 2011;3(2):166–79.

8. Lauffer BEL, Mintzer R, Fong R, Mukund S, Tam C, Zilberleyb I, et al. Histone deacetylase (HDAC) inhibitor kinetic rate constants correlate with cellular histone acetylation but not transcription and cell viability. J Biol Chem. 2013;288(37):26926–43.

9. Wang DF, Helquist P, Wiech NL, Wiest O. Toward selective histone deacetylase inhibitor design: Homology modeling, docking studies, and molecular dynamics simulations of human class I histone deacetylases. J Med Chem. 2005;48(22):6936–47.

10. Marks PA. Discovery and development of SAHA as an anticancer agent. Oncogene. 2007;26(9):1351–6.

11. Herman D, Jenssen K, Burnett R, Soragni E, Perlman SL, Gottesfeld JM. Histone deacetylase inhibitors reverse gene silencing in Friedreich's ataxia. Nat Chem Biol. 2006;2(10):551–8.

12. Beconi M, Aziz O, Matthews K, Moumné L, O'Connell C, Yates D, et al. Oral Administration of the Pimelic Diphenylamide HDAC Inhibitor HDACi 4b Is Unsuitable for Chronic Inhibition of HDAC Activity in the CNS In Vivo. PLoS One. 2012;7(9).

13. Attenni B, Ontoria JM, Cruz JC, Rowley M, Schultz-Fademrecht C, Steinkühler C, et al. Histone deacetylase inhibitors with a primary amide zinc binding group display antitumor activity in xenograft model. Bioorg Med Chem Lett. 2009;19(11):3081–4.

14. Pettersen EF, Goddard TD, Huang CC, Couch GS, Greenblatt DM, Meng EC, et al. UCSF Chimera-a visualization system for exploratory research and analysis. J Comput Chem. 2004;25(13):1605–12.

15. Berman HM, Westbrook J, Feng Z, Gilliland G, Bhat TN, Weissig H, et al. The Protein Data Bank www.rcsb.org. Nucleic Acids Res. 2000;28(1):235–42.

16. Bressi JC, Jennings AJ, Skene R, Wu Y, Melkus R, Jong R De, et al. Exploration of the HDAC2 foot pocket: Synthesis and SAR of substituted N-(2-aminophenyl)benzamides. Bioorg Med Chem Lett. 2010;20(10):3142–5.

17. Sulaiman GM, Jabir MS, Hameed AH. Nanoscale modification of chrysin for improved of therapeutic efficiency and cytotoxicity. Artif Cells, Nanomedicine Biotechnol. 2018;46(sup1):708–20.

18. Jabir MS, Taha AA, Sahib UI, Taqi ZJ, Al-Shammari AM, Salman AS. Novel of nano delivery system for Linalool loaded on gold nanoparticles conjugated with CALNN peptide for application in drug uptake and induction of cell death on breast cancer cell line. Mater Sci Eng C. 2019;94(March 2018):949–64.

19. Julian W. Hill. Studies On Polymerization And Ring Formation. VI. Adipic Anhydride. J Am Chem Soc. 1930;52:4110–4.

20. Letton JC, Miller LE. Process for the preparation of mono-condensation derivatives of adipic acid. US5286879A, 1994.

21. Stowell JC, Huot RI, Van Voast L. The Synthesis of N-Hydroxy-N′-phenyloctanediamide and Its Inhibitory Effect on Proliferation of AXC Rat Prostate Cancer Cells. J Med Chem. 1995;38(8):1411–3.

22. Wolfe S, Godfrey JC, Holdrege CT, Perron YG. Rearrangement of penicillins to anhydropenicillins. Can J Chem. 1968;46(15):2549–59.

23. Roe ET, Scanlan JT, Swern D. Fatty Acid Amides. I. Preparation of Amides of Oleic and the 9, 10-Dihydroxystearic Acids. J Am Chem Soc. 1949;71(6):2215–8.

24. Gorobets NY, Yermolayev SA, Gurley T, Gurinov AA, Tolstoy PM, Shenderovich IG, et al. Difference between 1H NMR signals of primary amide protons as a simple spectral index of the amide intramolecular hydrogen bond strength. J Phys Org Chem. 2012;25:287–95.